Void growth within hydrogels-a computational micro-scale analysis

M. DUBUS[a], L. SIAD[a], M. ELKOLLI-MERBAH[b], H. KERDJOUDJ[a], F.J. VERNEREY[c], D. LAURENT-MAQUIN[a], S.C. GANGLOFF[a]

a. BIOS, Université de Reims, UFR Pharmacie, 1 rue du Maréchal Juin, 51100 Reims, France.
larbi.siad@univ-reims.fr
b. LPMAMPM, Faculté de Technologie, Université Ferhat Abbas de Sétif-1, Algérie.
elkolli@hotmail.com
c. DME, University of Colorado, Boulder, Colorado 80309-0427, USA.
franck.vernerey@colorado.edu

Résumé :

La nature et les nombreuses caractéristiques remarquables des gels polymériques expliquent leur utilisation de plus en plus répandue comme biomatériaux en médecine régénératrice et en ingénierie tissulaire. Eu égard à leur biocompatibilité, leur déformabilité et leur grande capacité d'absorption de solvants, ces biomatériaux sont souvent sélectionnés en raison, notamment, de leurs propriétés mécaniques modulables et surtout proches de celles des tissus biologiques mous. Ce travail se propose d'étudier le comportement global de gels polymériques à l'intérieur desquels des microvides sont présents. Une tentative est mise en œuvre pour l'obtention d'une approximation des réponses macroscopiques de ces biomatériaux à des chargements proportionnels imposés. Dans cette perspective, la méthode d'homogénéisation à deux échelles proposée utilise un Volume Élémentaire Représentatif (VER) consitant en un simple cylindre axisymétrique constitué d'une matrice homogène imbibée de solvent et d'un vide sphérique en son centre. Les trajets de chargement imposés aux surfaces extérieures du VER sont tels que la triaxialité macroscopique est maintenue constante. Dans cette communication, les courbes contraintes-déformations macroscopiques, l'influence de la valeur de la porosité initiale, et celle de la triaxialité prescrite sont mises en évidence pour des valeurs fixées de la concentration du solvent et du paramètre d'interaction de Flory-Huggins.

Abstract :

The nature and the large notable distinguishing features of polymeric gels explain their pervasive use as biomaterials in both regenerative medicine and tissue engineering. With regard to their biocompatibility, their ability to withstand large deformation and their significant capacity of solvent absorption, these biomaterials are often selected owing to their versatile mechanical properties and especially the closeness to soft biological tissues, amongst others. The present work is undertaken in order to examine the overall behaviour of polymeric gels where microvoids are present. An attempt is made towards obtaining an estimation of their macroscopic responses to prescribed proportional loadings. To this end, a two-level representation of the material at hand for which the Representative Volume Element (RVE)

imbibed with a solvent is a simple axisymmetric cylinder composed of a homogeneous matrix surrounding a spherical void, is considered. The computational study addresses the situation where the RVE is subjected to prescribed axial and lateral overall stresses under conditions of constant overall stress triaxiality. In this communication, for fixed values of the Flory-Huggins parameter and the nominal concentration of the solvent, the overall stress-strain behaviour of the RVE model, the influence of the initial porosity, and the prescribed stress triaxiality ratio have been emphasized.

Mots clefs : gels ; hyperelasticity ; microvoid growth ; multiscale simulation ; polymeric biomaterials ; porosity ; swelling.

1 Introduction

Hydrogels are pervasive in biology and have been turned out to be nearly optimal for interfacing with dynamic systems. By way of illustration, they are used as biomaterials in order to enhance stem cell transplantation by addressing, in particular, the mechanical aspects associated with each stage of the transplantation process [2, 12]. The characteristic soft ability of these polymeric biomaterials makes them strongly resembling the extracellular matrix (ECM) which encapsulates cells in their native environment. Regarding tissue engineering, scaffolds made of hydrogels, just like ECM, act as a structural support and are able to accommodate biomechanical signals to control cell function and eventually their fate [9]. Nowadays, it is trite to claim that stem cells are known to respond to mechanical cues in their microenvironment by changing their morphology, dynamics, proliferation rate, migration speed, and differentiation potential [19, 7]. The physical process of mechanosensitivity is realized through the contact and adhesion between cells and their microenvironment [1].

Hydrogels, a cross-linked polymers immersed in a solvent (water), are an interesting class of materials that are able to undergo significantly large deformation which can also be triggered by external stimuli through appropriate change of constituents [18]. Solvent molecules migrate in a gel by self-diffusion. When hydrogels are subjected to mechanical loadings or also when the chemical potential of the environment changes, the polymer chain network deforms and the solvent molecules migrate to reach the thermodynamic equilibrium [20]. This equilibrium is reached as soon as the chemical potential of the solvent equals to that in the external solution. The mechanical, thermodynamic and kinetic properties of various environmentally sensitive hydrogels have been modeled and analyzed to study the different interesting phenomena exhibited, namely the phase transition and instability during swelling [14, 6, 3].

On the other hand, poor toughness of soft porous biomaterials may results in failure which is an issue of importance to both engineering and medical practice [16, 25, 4]. An understanding of failure mechanisms turns out to be crucial in the study of fracture of these biomaterials. Under sufficient loading, microvoids can be triggered inside materials as diverse as polymers, biological tissues, polymers, and even nominally pure materials [4]. As regard overall properties, the presence of those microscopic defects can have drastic consequences at the macroscopic level. By way of example, when those defects are accounted for the maximum pressure that an elastomeric solid can support changes from a theoretical infinite value for a

sound material to a finite one, [4, 29]. As a result, cavitation appears as soon as the void volume fraction suddenly and rapidly increases and, at the same time, the pressure approaches a critical value. Upon occurrence of such an event, unstable growth of microvoids in an elastic network may ultimately yield the failure of the considered material.

In addition to this, let us mention briefly that the toughness of a material depends on the ability of the microstructure to dissipate energy without propagation of defects like initiated microvoids or cracks [16, 25]. Subsequently, the understanding of failure mechanisms would also provide insight and afterwards enhancement into the production of tissue-engineering scaffolds with properly appropriate architecture and tailored properties. Scaffolds can be designed as porous structure (sponges) or in forms of hydrogels. Sponges facilitate cell adhesion and the pore size variation affects cell adhesion, migration and deposition. Hydrogels support the transportation of cells and bioactive agents and can suspend cells in a three dimensional environment. Keeping the focus on the porosity, among the essential characteristics that ideal scaffolds should share in order to be successful are the following [23, 22, 21] : i) the scaffolds should have high permeability to enable adequate diffusion of nutrients for the cells and the removal of waste products ; ii) the cell supports porosity should be sufficiently high to allow for the ingress of cells and provide the cells space to proliferate and form the ECM ; iii) they should have a large surface area ; and iv) the pore size should be fine-tuned to the cells type applied.

In this numerical study, the growth of a small spherical void within a polymeric gel is viewed through the prism of micromechanics [24, 8, 10] and finite element analysis. A two-level representation of the material at hand is considered. The mesoscopic scale is treated through an axisymmetric representative volume element (RVE) composed of two phases : a homogeneous void free matrix and spherical void. The behaviour of the RVE is appropriately averaged to provide the so-called macroscopic behaviour of the material considered as homogeneous. The calculations are very similar to many earlier similar simulations, the prototype of which is due to Koplik and Needleman [17]. The boundary conditions of the RVE are prescribed under proportional stressing in such a way that the isotropically invariant stress triaxiality keeps a constant prescribed value throughout the loading displacement controlled history.

2 Governing equations

The problem formulation and material modelling of hydrogels are briefly presented in this section. Closely following works in [14, 15, 28], the governing equations and corresponding boundary conditions for equilibrium swelling deformation of this material are described. They serve as the basis for the numerical studies presented in the subsequent sections.

2.1 Kinematics and balance equations of finite growth

Consider a hydrogel body (current state) of volume Ω enclosed by a surface Γ, subjected to body force, $\underline{\mathbf{b}}$, and surface traction, $\underline{\mathbf{t}}$. Due to immersion of the hydrogel body in a solvent environment of chemical potential μ (per solvent molecule), a transport of the solvent molecules occurs within Ω and across Γ. In addition, part of the surface Γ may be mechanically constrained (*e.g.*, bounded to a rigid body) and/or chemically isolated from the solvent. Due

to large deformation, it is more appropriate to use nominal quantities referring to a reference state with fixed volume Ω_o and surface Γ_o. A generic material particle occupying position $\underline{\mathbf{X}}$ at the reference state moves to position $\underline{\mathbf{x}}(\underline{\mathbf{X}}, t)$ at the current state at time t. The deformation gradient tensor maps both reference states, namely,

$$F_{iK} = \frac{\partial x_i(\underline{\mathbf{X}}, t)}{\partial X_K} \quad \text{with} \quad J := \det \underline{\underline{\mathbf{F}}} > 0 \tag{1}$$

While the choice of the reference state is arbitrary in general, we choose the dry state of the hydrogel as the reference state in the present study. Such a choice is necessary for the use of a specific free energy function. However, let us mention from now that a numerical challenge has to be circumvented in finite element analysis by using an intermediate configuration for which $J \neq 1$. The equation of force balance in terms of the nominal stress $\underline{\underline{\mathbf{s}}}$ and boundary conditions can be set as follows

$$\frac{\partial s_{iK}(\underline{\mathbf{X}}, t)}{\partial X_K} + B_i(\underline{\mathbf{X}}, t) = 0 \quad \text{and} \quad \underline{\mathbf{X}} = \bar{\underline{\mathbf{X}}} \text{ or } s_{iK} N_K = \bar{T}_i^o \tag{2}$$

where $\bar{\underline{\mathbf{T}}}^o$ is traction per unit area of the reference surface with the unit outward normal $\underline{\mathbf{N}}$ and the barred quantities are prescribed. In the circumstance of absence of any chemical reaction, the conservation of the number of injected small molecules at the chemical potential μ into the gel, in the vicinity of $\underline{\mathbf{X}}$, read

$$\frac{\partial C(\underline{\mathbf{X}}, t)}{\partial t} + \frac{\partial J_K(\underline{\mathbf{X}}, t)}{\partial X_k} = r(\underline{\mathbf{X}}, t) \tag{3}$$

where r is the number of the small molecules per unit time injected into a volume element dV, $J\, N_K\, dA$ is the number of the small molecules per unit time crossing an element of area $\underline{\mathbf{N}}\, dA$, and C be the concentration of the solvent number. The polymers and the individual small molecules are assumed to be incompressible, which is reflected in the incompressibility condition

$$1 + v\, C(\underline{\underline{\mathbf{F}}}, C) = J \tag{4}$$

where v is the volume per small molecule and $v\, C$ is the volume of the small molecules in the gel divided by the volume of the dry polymers.

2.2 Constitutive equations

Standard reasoning in thermodynamics accounting for condition of molecular incompressibility through the use of a field of Lagrange multiplier Π results in (refer to, *e.g.*, [6, 13, 27] and also to above mentioned references)

$$s_{iK} = \frac{\partial W(\underline{\underline{\mathbf{F}}}, C)}{\partial \underline{\underline{\mathbf{F}}}} - \Pi\, J H_{iK} \quad , \quad \mu = \frac{\partial W(\underline{\underline{\mathbf{F}}}, C)}{\partial C} + \Pi\, v \tag{5}$$

where W is the free energy of the gel and $\underline{\underline{\mathbf{H}}}$ is the transpose of the inverse of the deformation gradient $\underline{\underline{\mathbf{F}}}$, , namely, $H_{iK} F_{iL} = \delta_{KL}$ and $H_{iK} F_{jK} = \delta_{ij}$ [1].

1. Algebraic identity : $\dfrac{\partial (\det \mathbf{F})}{\partial F_{iK}} = \det \mathbf{F} H_{iK}$

For the dissipation due to solvent migration, we can correlate the solvent flux, **J**, to its driving force, the chemical potential gradient, as

$$\mathbf{J} = -\mathbf{M}\boldsymbol{\nabla}_x \mu \tag{6}$$

The spatial differential operator $\boldsymbol{\nabla}_x$ is taken with respect to the reference configuration. The kinetic tensor **M** may not be constant in general, but is all positively definite.

The choice of an explicit form of the free-energy function W for elastomers and soft tissues is a controversial problem. This choice is needed in order to solve the initial value problem under consideration. Following Flory and Rehner [11], W has the form $W(\underline{\underline{\mathbf{F}}}, C) = W_s(\underline{\underline{\mathbf{F}}}, C) + W_m(C)$ reflecting the stretching network of the polymers, W_s, and the mixing of the polymers and the small molecules, W_m. These two terms are taken to be

$$\begin{aligned} W_s(\underline{\underline{\mathbf{F}}}, C) &= \frac{1}{2} NkT(F_{iK}F_{iK} - 3 - 2\log J) \\ W_m(C) &= -\frac{kT}{v}\left[vC log\left(1 + \frac{1}{vC}\right) + \frac{\chi}{1+vC}\right] \end{aligned} \tag{7}$$

where N is the number of polymer chains in the gel per unit volume of the dry polymers, v is the volume per solvent molecule, T is the absolute temperature, and k is the Boltzmann constant. The first term inside the bracket comes from the entropy of mixing, and the second from the enthalpy of mixing. The Flory interaction parameter χ is a dimensionless measure of the enthalpy of mixing, with representative values $\chi = 0 - 1.2$. For applications that prefer gels with large swelling ratios, materials with low χ values are used. The enthalpy of mixing motivates the small molecules to enter the gel if $\chi < 0$, but motivates the small molecules to leave the gel if $\chi > 0$. The chemical potential and stresses are normalized by kT and kT/v, respectively. The material properties of the hydrogel is fully determined by three parameters : NkT, $\frac{kT}{v}$, and χ. The first two combine to give one dimensionless parameter, Nv. It is well known that NkT defines the initial shear modulus of the polymer network, with the number N proportional to the crosslink density ρ_c,[27, 26]. A representative value of the volume per molecule is $v = 10^{-28}\,\mathrm{m}^3$. At room temperature, $kT = 4 \times 10^{-21}\,\mathrm{J}$ and $kT/v = 4 \times 10^7\,\mathrm{Pa}$. In the numerical examples below, we will take the values $Nv = 10^{-3}$ and $\chi = 1.2$. The normalized chemical potential is mimicked by a temperature-like variable, which is uniform in the polymeric gel, and is incremented as a loading parameter. The whole governing equations and the thorough approach have been implemented into Abaqus via a UHYPER subroutine. [14, 15, 28].

3 The axisymmetric RVE model

The voids are assumed to be uniformly distributed inside the matrix material as shown in Figure 1-a. Specifically, the position of these voids are presumed to form a hexagonal crystal lattice in such a way that the shape of the unit microstructure is a prism with hexagonal basis face with inner radius R_o, height $2\,L_o$, and containing an initially spherical void with radius r_o. In order to reduce the effort of calculations to a two-dimensional analysis, the cross section of the unit microstructure has been simplified as a cylinder, as done in [5, 17]. Due to this approximation, the axisymmetric RVE is shown in Figure 1-d for which a

cylindrical reference coordinate system with radial coordinate R, circumferential angle Θ and axial coordinate Z is used for the analysis. In the initial undeformed configuration, the RVE model is a cylinder with diameter $2\,R_o$ and height $2\,L_o = 2\,R_o$ (for the sake of simplicity). The initial axisymmetric RVE geometry is then simply characterized by the initial void volume fraction f_o given by $f_o = \frac{2}{3}\left(\frac{r_o}{R_o}\right)^3$. The RVE model is assumed to be subjected to axisymmetric deformations with constant prescribed overall triaxiality so that all field quantities are independent of Θ.

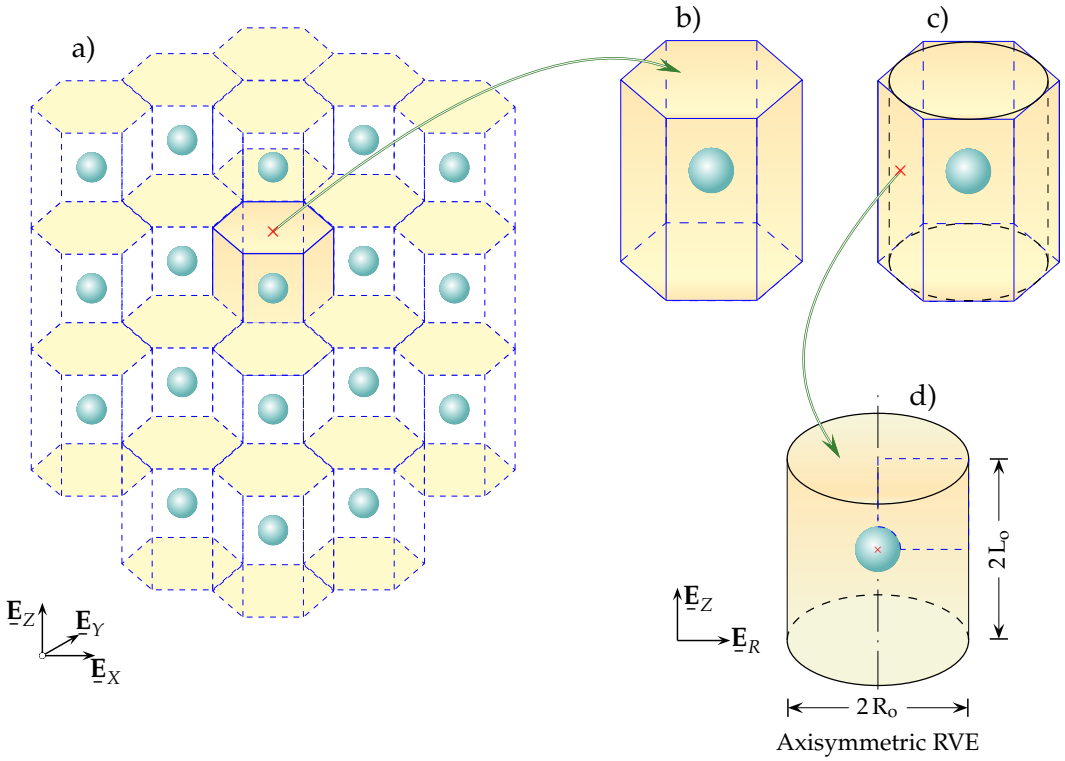

FIGURE 1 – Three-dimensional hexagonal arrangement of spherical voids. a) Schematic representation of a porous polymeric gel which is considered as an array of unit hexagonal RVEs, each containing a single spherical void. The porous unit hexagonal microstructure shown in (b) is approximated by the axisymmetric RVE model displayed in (d).

As a consequence of the lattice periodicity all outer planes of the unit cell have to move as rigid planes in coordinate directions during the process of loading (Figure 2). The faces at $R = R_o$ and $Z = L_o$ will have a uniform normal displacements and their mutual orientations will be maintained. These requirements impose the RVE model to remain, during the finite strain deformation process, a cylinder which is thus characterized in an arbitrary state by $\ell_R = R_o + u_R^A$ and $\ell_Z = L_o + u_Z^A$ where u_R^A and u_Z^A are the radial and axial components displacement of the upper right corner **A**. Because of these constraints, only one quarter geometry of the RVE model ($0 \leq R \leq R_o$, $0 \leq Z \leq L_o$) needs to be analyzed and is drawn in Figure 2.

The overall deformation of the RVE model can be calculated from the normal displacements of the outer faces. The macroscopic total logarithmic strain tensor and Cauchy stress tensor possess the same principal directions, which are the radial and axial directions. The effective strain E_e defined by $E_e = \frac{2}{3}\,|E_Z - E_R|$ where E_R and E_Z are the macroscopic principal strains, is chosen as the overall deformation of the RVE model and the independent variable for

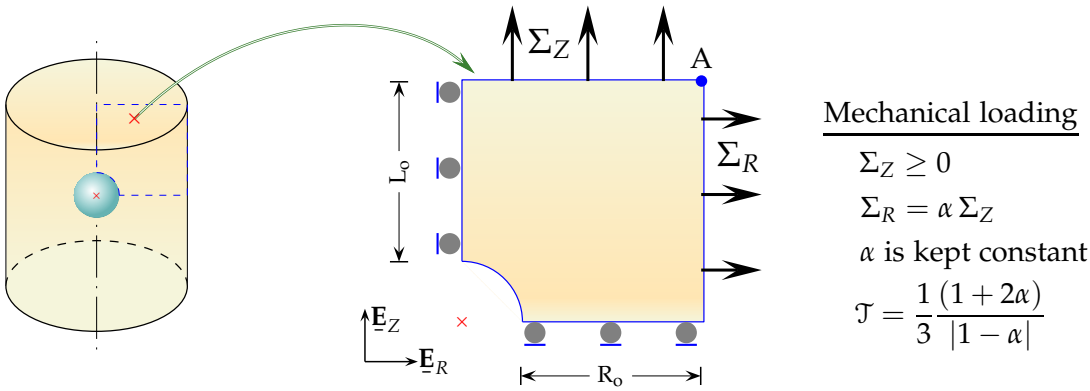

FIGURE 2 – Axisymmetric RVE model containing an isolated spherical void and to be FE analyzed.

presenting most results. The effective von Mises stress Σ_e , hydrostatic stress Σ_h, and the overall stress triaxiality $\mathcal{T}$ result from

$$\Sigma_e = |\Sigma_Z - \Sigma_R| \ , \ \Sigma_h = \frac{1}{3}(\Sigma_Z + 2\Sigma_R) \ , \ \mathcal{T} := \frac{\Sigma_h}{\Sigma_e} = \frac{1}{3}\frac{(\Sigma_Z + 2\Sigma_R)}{|\Sigma_Z - \Sigma_R|} \tag{8}$$

where Σ_R is the remote macroscopic principal stresses in both R and Θ directions, and Σ_Z in the Z-one. The RVE model is presumed to be remotely loaded with predominant axial stress; that is the axial direction is assumed to be the maximum principal direction and the components of the overall stress tensor $\underline{\underline{\Sigma}}$ are then such that $\Sigma_Z \geq \Sigma_R$.

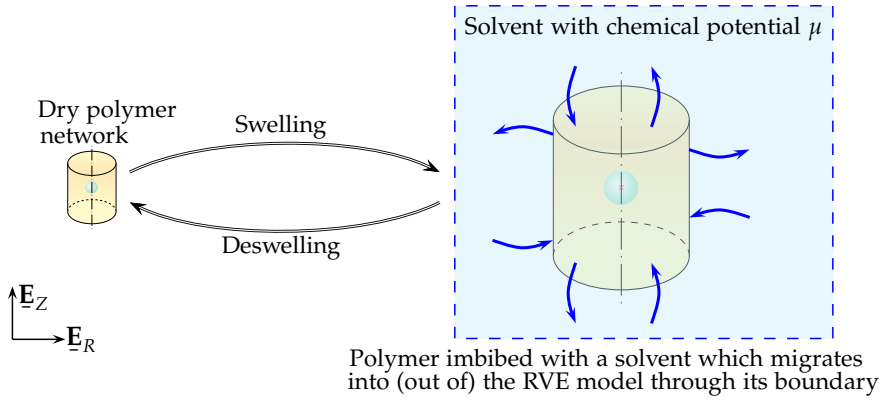

FIGURE 3 – Swelling-deswelling of the axisymmetric RVE model. After swelling the porosity is maintained constant.

For metal, it is a well known fact that the stress triaxiality ratio $\mathcal{T}$ is the most important driving force to void growth in porous materials [5, 17]. On that account, a general problem in RVE model computations is to maintain $\mathcal{T}$ constant in the course of loading irrespective of the large displacement of the cell faces and the unstable stiffness behaviour. The finite elements used were eight-nodes quadrilateral isoparametric elements. The mesh surrounding the void is slightly refined and it was judged to be sufficiently refined for this study (800 Q8 elements). Care has been taken to insure that the meshes were sufficiently refined and that the results were independent of the degree of refinement. The Riks's arc-length method in Abaqus is used in order to handle the inevitable instability of the RVE and to proceed with further calculations. The overall stress and strain rates are directly computed from the reaction forces

and the applied displacement rates. The actual void volume fraction f corresponding to the evolution of the microvoid is calculated using numerical integration from the updated coordinates of the nodes at the void-matrix interface during the deformation of the RVE model. The initial conditions and loading rate of the RVE model are chosen such that inertial effects are negligible. No artificial damping has been used in all computations. The value of the imposed axial displacement u_z^A depends essentially upon the value of f_o and the fixed stress triaxility $\mathcal{T}$ as well. In addition, the imposed boundary conditions have to be ramped up using a function of time over the first part of calculation (typically the first 1-10%).

4 Numerical results

For the simulation presented hereafter, the chosen hydrogel properties are the following : initial polymer volume fraction $\phi_o = 0.90$, degree of cross-linking $Nv = 0.0010$, and parameter $\chi = 0.10$. At the reference state corresponding to an initially swollen hydrogel of properties ϕ_o, Nv and χ, its initial chemical potential is prescribed by μ_o/kT given by $\mu_o/kT = Nv(\phi_o^{1/3} - \phi_o) + \ln(1-\phi_o) + \phi_o + \chi\phi_o^2 = -1.3216$. This prescribed value is accounted for in Abaqus as an initial condition [28]. The porosity f_o takes on values $0.10, 0.50, 1.0, 2.0, 5.0$ and $10.0\,\%$. $\mathcal{T}$ ranges from $\frac{1}{3}$ (pure tension) to 2 (severe stress state for soft materials). However, in the interest of place only the value $f_o = 5.0\,\%$ is considered.

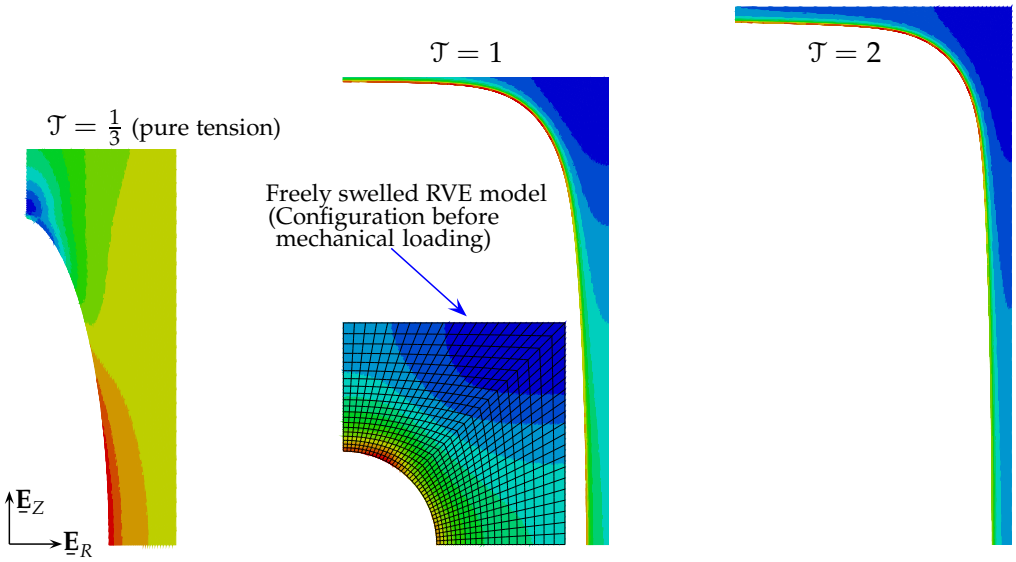

FIGURE 4 – Distribution of lagrangian strain component LE_{22} at the end of calculations and final deformation shape of the RVE model for $f_o = 5.0\%$. The hydrogel properties are $\phi_o = 0.90$, $Nv = 0.0010$, and $\chi = 0.10$. The mechanical loading of the freely swelled RVE model has been performed under constant stress triaxiality ratio $\mathcal{T} = \frac{1}{3}$ (a), 1 (b), and 2 (c).

The swelling-mechanical loading of the RVE model at hand may be summarised as follows :

- the polymer network of the RVE model with initial porosity f_o is first imbibed with solvent as shwn in Figure 3. Subsequently, homogeneous swelling occurs and the size of the RVE model changes a lot irrespective of the value of f_o. At equilibrium the chemical potential μ is homogeneous throughout the RVE model which porosity after swelling turns out to be practically equal to f_o.

- The swelled RVE model is then subjected to axial and lateral overall stresses under conditions of constant prescribed overall stress triaxiality.

Contour plots of the lagrangian strain component LE_{22} are shown in Figure 4 corresponding to $\mathcal{T} = \frac{1}{3}, 1, 2$, respectively. For each initial porosity f_o and for each value of the overall stress triaxiality $\mathcal{T}$, the evolution of the normalized effective stress, $\frac{\Sigma_e}{kT}$ and the porosity f are displayed in Figure 5 as a function of the equivalent strain E_e.

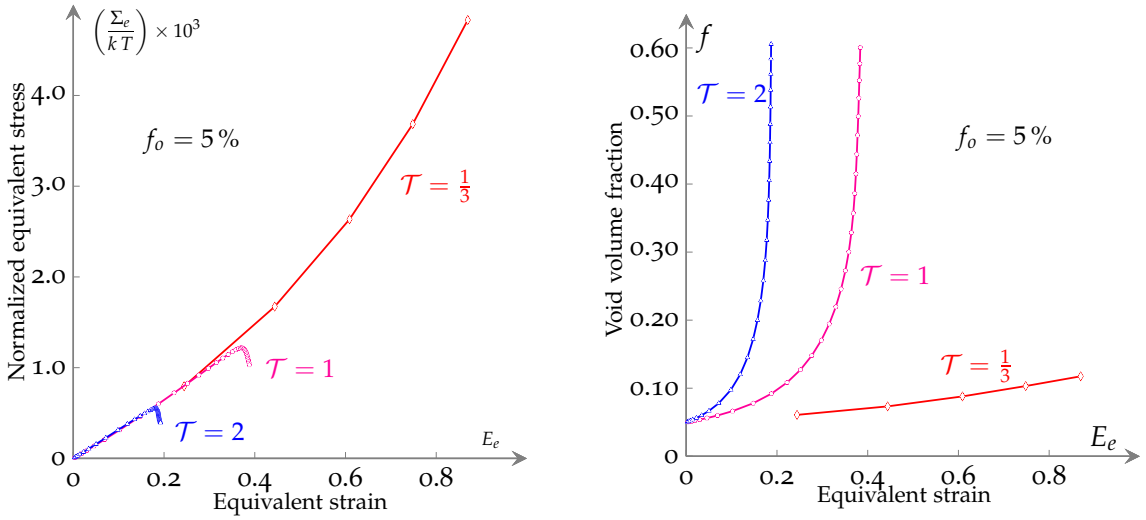

FIGURE 5 – Evolution of the normalized equivalent stress $\frac{\Sigma_e}{kT}$ and the void volume fraction f in terms of the macroscopic equivalent strain E_e of the RVE model. The initial value of the void volume fraction is 5.0 % and the stress triaxiality $\mathcal{T}$ is fixed to be $\frac{1}{3}$, 1 and 2.

As an illustration, Figure 6 shows the deformation of the RVE model and evolution during the whole process of loading of the lagrangian strain component LE_{22} contours for $f_o = 0.10\,\%$ and $\mathcal{T} = 1$. The corresponding curves $(\frac{\Sigma_e}{kT}, E_e)$ and (f, E_e) are shown in Figure 7 from which one can observe that beyond the peak stress ($E_e = 0.53$, $(\frac{\Sigma_e}{kT})^{max} = 2.35 \times 10^{-3}$, and $f = 0.17$) the void volume fraction increases very quickly.

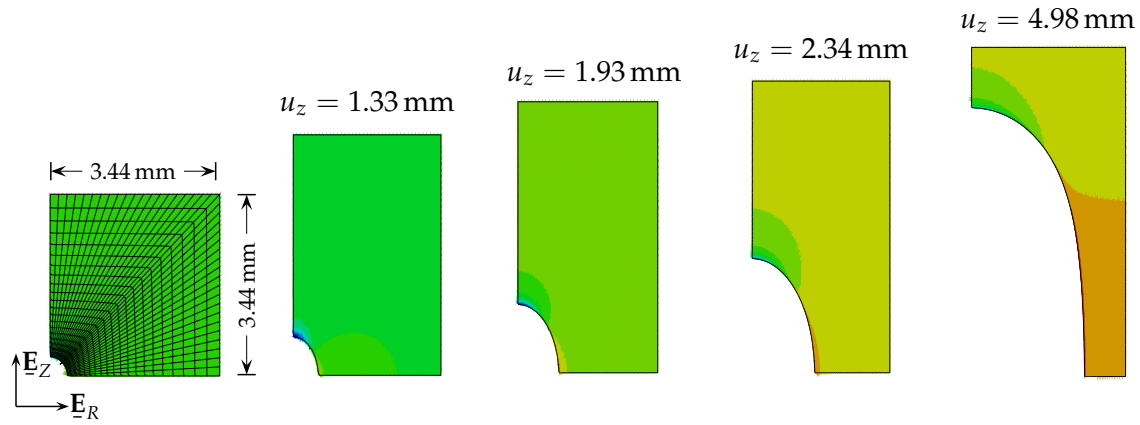

FIGURE 6 – Deformation of the RVE model and evolution of contours of the lagrangian strain component LE_{22} for $f_o = 0.10\,\%$ and $\mathcal{T} = 1$. The hydrogel properties are $\phi_o = 0.90$, $Nv = 0.0010$, and $\chi = 0.10$.

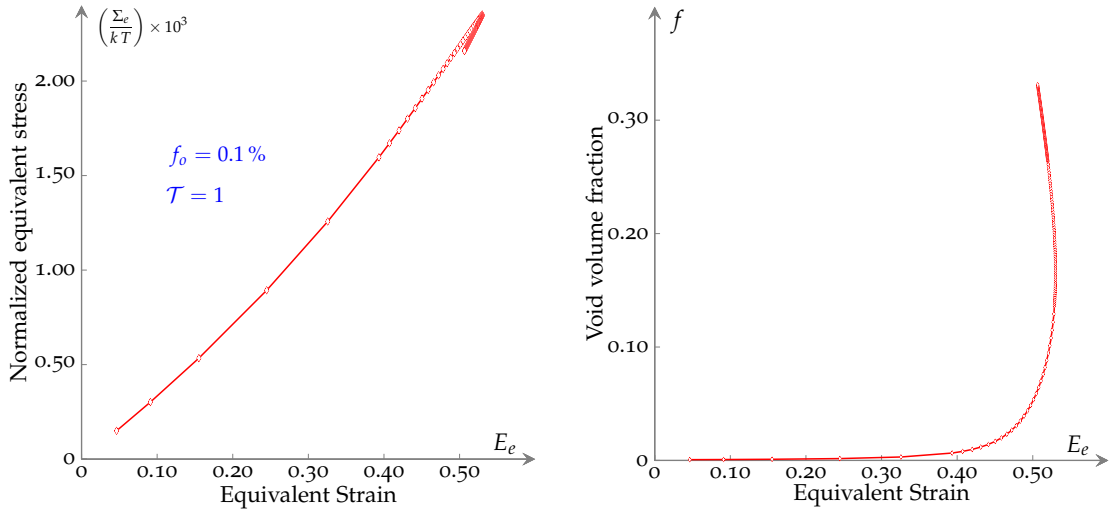

FIGURE 7 – Evolution, for $\mathcal{T} = 1$, of the normalized effective stress and the void volume fraction in terms of the macroscopic effective strain E_e of the RVE model.

5 Concluding remarks

This study focuses on the mechanical behaviour of porous polymeric gels intended for use in tissue engineering and regenerative medicine as scaffolds ldots. Following Hong *et al.* [14] and Koplik and Needleman [17], we present a computational framework for investigating the growth of microvoids initially assumed to be spherical and uniformly distributed inside the matrix material. In this preliminary investigation the swollen axisymmetric RVE is viewed as a two-component body composed of two incompressible components, namely, an elastic polymer and a solvent. The distribution of the solvent is assumed to be uniform and then the state of the RVE is fully characterized by the radius of the central spherical microvoid. Under the conditions that i) the ambient chemical potential of the solvent is fixed, ii) the chemical equilibrium prevails at the interface between the polymer and the environment interface, and iii) the mechanical loading of the RVE is such that the stress triaxiality ratio is maintained constant throughout the whole process of deformation. The evolution of the size and the shape of the microvoid has been obtained. From this preliminary study, the following conclusions are drawn.

- For a porous polymeric gel, the amount of solvent molecules inside the material is related to the chemical potential of the environment. The degree of swelling is obtained by solving equations that account for the simultaneous interaction of mechanics and absorption. It can be determined with a free swelling stretch, using a finite element analysis.
- As an expected result, the value of initial porosity has a large influence on the overall mechanical behaviour of a porous polymeric gel. Higher the initial value of the void volume fraction, lower the resistance (maximum effective stress) of the polymeric gel.
- The size of the swollen axisymmetric porous RVE model does not depend on the initial value of the porosity and the void volume fraction is kept constant after swelling.
- For moderate stress triaxiality (*e.g.*, $\mathcal{T} = \frac{1}{3}$ corresponding to a tensile test), the effective stress Σ_e continuously increases with equivalent strain E_e. The same applies to the variations of void volume fraction f in terms of E_e, (red curves in Figure 5).
- For high stress triaxiality, the curves normalized effective stress *vs* equivalent strain display maximum depending on both the initial porosity and the fixed value of the overall

triaxiality. For $\mathcal{T} = 1$ and 2, beyond macroscopic peak stresses, the void volume fraction rapidly increases, (magenta and blue curves in Figure 5).

The prevalent approach of modeling the porous biomaterial at hand as an assemblage of axisymmetric unit RVEs reduces the amount of work required for the multiscale analysis. This convenience comes with an approximation since this assemblage cannot patently fill the space continuously, and then is only suited for moderate porosity. Furthermore, the used axisymmetric RVEs do not allow the adjustment of arbitrary stress ratios in three directions. Otherwise, it is clear from the previous simulation that special care would be considered after maximum load occur in the vicinity of the boundary of void. Indeed, it is well known that strong softening of the material result in localized deformation and consequently the mesh size dependence. After the peak macroscopic stresses the equivalent stress drops abruptly and the validity of the numerical results is expected to quickly deteriorate because of mesh excessive distortion. Finally, so far for the analysis presented above a criterion for the final failure of the intervoid ligament is clearly missing.

The fact of the matter is that this preliminary study could be of some relevance in regard to failure of responsive polymeric gels. Numerous tissues and organs are hydrogel-like in nature and several issues related to the mechanics of hydrogels remain open (a short list is given in the review [20]). With increment of biomedical applications, computational modelling to predict the performance of these biomaterials for use in regenerative medicine and tissue engineering proves to be a valuable aid in assisting understanding of the behaviour of hydrogels and their optimization as well. The investigation of the effects of the constitutive parameters entering the theory, namely, the number N of polymer chains per unit volume of the dry polymers, the volume per solvent molecule v, and the Flory interaction parameter χ, on the overall behaviour of a porous polymeric gel are contemplated as a future research work.

Références

[1] U. Akalp, C. Schnatwinkel, M.P. Stoykovich, S.J. Bryant, F. J. Vernerey,, Structural Modeling of Mechanosensitivity in Non-Muscle Cells : Multiscale Approach to Understand Cell Sensing, ACS Biomaterials Sci. Eng., 3 (2017), p. 9.

[2] G.M. Artmann, S. Chien, (eds), Bioengineering in Cell and Tissue Research, Springer, Heidelberg, Berlin, 2008.

[3] S. Baek, A.R. Srinivasa, A thermo-mechanically coupled theory for fluid permeation in elastomeric materials, Int. J. Nonlinear Mechanics, 39 (2004), 201-2018.

[4] J.M. Ball, Discontinuous equilibrium solutions and cavitation in nonlinear elasticity, Phil. Trans. Royal Soc., London. Series A, (1982) 557–611.

[5] W. Brocks W., D.Z. Sun, A. Hönig, Micromechanics of coalescence in ductile fracture, Int. J. Plasticity, 11 (1995), 971-989.

[6] A.S. Chester, L. Anand, A thermo-mechanically coupled theory for fluid permeation in elastomeric materials, J. Mech. Phys. Solids, 59 (2011), 1966-2006.

[7] D. Disher *et al.*, Biomechanics : Cell research and applications for the next decade, Annals of Biomedical Engineering, 37 (2009), 847–859.

[8] L. Dormieux, D. Kondo, F.-J. Ulm, Microporomechanics, John Wiley & Sons, Ltd., Chichester, 2006.

[9] P.R. Fernandes, P.J. Bártolo, (eds), Tissue Engineering : Computer Modeling, Biofabrication and Cell Behavior, Springer, Dordrecht, Heidelberg, 2014.

[10] J. Fish, Practical Multiscaling, John Wiley & Sons Ltd., Chichester, 2014.

[11] P.J. Flory, J. Rehner,. Statistial mechanics of cross-linked polymer networks II. Swelling, J. Chem. Phys., 11 (1943), 521–526.

[12] A.A. Foster, L.M. Marquardt, S.C. Heilshorn, The diverse roles of hydrogel mechanics in injectable stem cell ... Current Opinion in Chemical Engineering, 15 (2017), 15-23.

[13] G.A. Holzapfel, R.W. Ogden, (eds.), Mechanics of Biological Tissue, Springer, Berlin, Heidelberg, 2006.

[14] W. Hong, Z.S. Liu, Z.G. Suo, Inhomogeneous swelling of a gel in equilibrium with a solvent and mechanical load, Int. J. Solids Structures, 46 (2009), 3282-3289.

[15] M.K. Kang, R. Huang, A variational approach and FE implementation for swelling of polymeric hydrogels ..., Journal of Applied Mechanics, 77 (2010), 061004.

[16] C.T. Koh, D.G.T. Strange, K. Tonsomboon, M.L. Oyen, Failure mechanisms in fibrous scaffolds, Acta Biomaterialia, 9 (2013), 7326-7334.

[17] J. Koplik, A. Needleman, Void growth and coalescence in porous plastic solids, Int. J. Solids Structures, 24 (1988), 835–853.

[18] H. Li, Smart Hydrogel Modelling, Springer, Dordrecht, 2009.

[19] X. Zheng, S. Li, S.S. Kohles, Multiscale Biomechanical Modeling of Stem Cell-Extracellular Matrix Interactions, in : S. Li and B. Sun, (eds.), Advances in Cell Mechanics, Chapter 2, Springer, Heidelberg, 2011, pp. 27-53.

[20] Z.S. Liu, W. Toh, T.Y. Ng, Advances in mechanics of soft materials : large deformation behavior of hydrogels, Int. J. Appl. Mech., 7 (2015), 35.

[21] P.X. Ma, Scaffolds for tissue fabrication, Materialstoday, 7 (2004), 30-40.

[22] C. Mauli Agrawal, J. L. Ong, M.R. Appleford, G. Mani Introduction to Biomaterials, Cambridge University Press, Cambridge UK, 2014.

[23] C. Migliaresi, A. Motta, (Eds), Scaffolds for Tissue Engineering. Biological Design, Materials, and Fabrication, Pan Stanford Publishing Pte. Ltd., Singapore, 2014.

[24] S. Nemat-Nasser, M. Hori, Micromechanics : overall properties of heterogeneous materials, North-Holland, Elsevier, Amsterdam, 2nd edition, 1999.

[25] J.A. Stella, A. D'Amore, W.R. Wagner, M. S. Sacks, On the biomechanical function of scaffolds for engineering load-bearing ..., Acta Biomaterialia, 6 (2010), 2365-2381.

[26] L.R.G. Treloar, The Physics of Rubber Elasticity, Oxford University Press, Oxford, 1975.

[27] K. Volokh, Mechanics of Soft Materials, Springer, Singapore, 2016.

[28] W.H. Wong, Instability study of soft materials-Modelling and simulation, PhD thesis, National University of Singapore, Singapore, 2011.

[29] J.A. Zimberlin, G.N. Tew, N. Sanabria-Delong, A.J. Crosby, Cavitation rheology fo soft materials, Soft Matter, 3 (2007), 763–767.